AGU PUBLICATIONS

JGR

Journal of Geophysical Research: Atmospheres

RESEARCH ARTICLE
10.1002/2016JD025688

Special Section:
Studies of Emissions and Atmospheric Composition, Clouds and Climate Coupling by Regional Surveys, 2013 (SEAC4RS)

In situ measurements of water uptake by black carbon-containing aerosol in wildfire plumes

Anne E. Perring[1,2], Joshua P. Schwarz[1], Milos Z. Markovic[1,2,3], David W. Fahey[1], Jose L. Jimenez[2,4], Pedro Campuzano-Jost[2,4], Brett D. Palm[2,4], Armin Wisthaler[5,6], Tomas Mikoviny[5], Glenn Diskin[7], Glen Sachse[7], Luke Ziemba[7], Bruce Anderson[7], Taylor Shingler[8], Ewan Crosbie[8,9], Armin Sorooshian[8,10], Robert Yokelson[11], and Ru-Shan Gao[1]

[1]Chemical Sciences Division, NOAA Earth System Research Laboratory, Boulder, Colorado, USA, [2]Cooperative Institute for Research in the Environmental Sciences, University of Colorado Boulder, Boulder, Colorado, USA, [3]Now at Picarro Inc., Toronto, Ontario, Canada, [4]Department of Chemistry and Biochemistry, University of Colorado Boulder, Boulder, Colorado, USA, [5]Department of Chemistry, University of Oslo, Oslo, Norway, [6]Institute for Ion Physics and Applied Physics, University of Innsbruck, Innsbruck, Austria, [7]NASA Langley Research Center, Hampton, Virginia, USA, [8]Department of Chemical and Environmental Engineering, University of Arizona, Tucson, Arizona, USA, [9]Now at NASA Langley Research Center, Hampton, Virginia, USA, [10]Department of Hydrology and Atmospheric Sciences, University of Arizona, Tucson, Arizona, USA, [11]Department of Chemistry, University of Montana, Missoula, Montana, USA

Abstract Water uptake by black carbon (BC)-containing aerosol was quantified in North American wildfire plumes of varying age (1 to ~40 h old) sampled during the SEAC[4]RS mission (2013). A Humidified Dual SP2 (HD-SP2) is used to optically size BC-containing particles under dry and humid conditions from which we extract the hygroscopicity parameter, κ, of materials internally mixed with BC. Instrumental variability and the uncertainty of the technique are briefly discussed. An ensemble average κ of 0.04 is found for the set of plumes sampled, consistent with previous estimates of bulk aerosol hygroscopicity from biomass burning sources. The temporal evolution of κ in the Yosemite Rim Fire plume is explored to constrain the rate of conversion of BC-containing aerosol from hydrophobic to more hydrophilic modes in these emissions. A BC-specific κ increase of ~0.06 over 40 h is found, fit well with an exponential curve corresponding to a transition from a κ of 0 to a κ of ~0.09 with an *e*-folding time of 29 h. Although only a few percent of wildfire particles contain BC, a similar κ increase is estimated for bulk aerosol and the measured aerosol composition is used to infer that the observed κ change is driven by a combination of incorporation of ammonium sulfate and oxidation of existing organic materials. Finally, a substantial fraction of wildfire-generated BC-containing aerosol is calculated to be active as cloud condensation nuclei shortly after emission likely indicating efficient wet removal. These results can constrain model treatment of BC from wildfire sources.

Key Points:
- BC particles in wildfire plumes are found to be thickly coated with low hygroscopicity materials (ensemble average κ of 0.04)
- Hygroscopicity of BC-containing particles increases in an evolving plume due to incorporation of ammonium sulfate and oxidation of organics
- A substantial fraction of wildfire-generated BC-containing aerosol is calculated to be CCN active shortly after emission

Supporting Information:
- Supporting Information S1

Correspondence to:
A. E. Perring,
Anne.Perring@noaa.gov

Citation:
Perring, A. E., et al. (2017), In situ measurements of water uptake by black carbon-containing aerosol in wildfire plumes, *J. Geophys. Res. Atmos.*, *122*, 1086–1097, doi:10.1002/2016JD025688.

Received 22 JUL 2016
Accepted 6 DEC 2016
Accepted article online 12 DEC 2016
Published online 20 JAN 2017

1. Introduction

Black carbon (BC)-containing aerosol is the primary aerosol absorber of short-wave solar radiation in the atmosphere and has a positive climate forcing second only to that of carbon dioxide [*Bond et al.*, 2013]. Despite this importance, the processes governing the lifetime and distribution of BC in the atmosphere remain poorly characterized. Several recent papers have highlighted the difficulty of modeling BC loadings in the remote atmosphere [*Schwarz et al.*, 2013, 2010; *Shen et al.*, 2014; *Wang et al.*, 2014], which has been attributed, in part, to parameterization of BC removal. The modeled atmospheric lifetime of BC is highly sensitive to uncertainties in both the amount of non-refractory material internally mixed with BC (here referred to generically as "coatings") and interactions of BC-containing aerosol with water in the atmosphere. BC, a refractory material with a vaporization temperature near 4000 K [*Moteki and Kondo*, 2010], is chemically inert and insoluble; thus, water uptake by BC-containing particles is driven by the hygroscopicity of internally mixed materials. The presence of coatings on, and water uptake by, BC-containing aerosol can enhance BC light absorption by up to a factor of 1.6, [*Moffet and Prather*, 2009] resulting in additional uncertainties in calculations of direct radiative forcing.

BC is introduced to the atmosphere through various forms of combustion including controlled combustion of fossil and biofuels and uncontrolled open combustion of biomass. These different sources can generate BC-containing particles with markedly different microphysical characteristics affecting their atmospheric

processing and loss processes. BC produced by controlled fossil fuel combustion is typically fairly small and bare, causing it to be initially hydrophobic [*Dusek et al*., 2006; *Koehler et al*., 2009] while becoming more hygroscopic with atmospheric aging due to accumulation of water-active coatings [*Petters et al*., 2006; *Zhang et al*., 2008]. In less efficient open combustion sources, on the other hand, BC is coemitted with a wide suite of condensable species generating relatively large BC that is thickly coated shortly after emission [*Schwarz et al*., 2008]. A few recent studies have investigated factors affecting BC removal rates; *Moteki et al*. [2012] and *Taylor et al*. [2014] report size-dependent removal of BC in air parcels that have undergone wet scavenging, and *Zhang et al*. [2015] infer, based on remote atmosphere comparisons between modeled and measured BC loadings, that the average BC lifetime varies from less than 1 day to more than a week depending on the source region, season, and latitude. Nonetheless, inferred or prescribed rates of BC conversion from hydrophobic to hydrophilic modes in global models vary widely [*Cape et al*., 2012; *Chung and Seinfeld*, 2002; *Cooke and Wilson*, 1996; *Samset et al*., 2014] and are rarely constrained by direct observation of BC aerosol hygroscopicity. This uncertainty strongly impacts model skill in accurately reproducing the global burden of BC aerosol and the associated radiative impacts [*Bond et al*., 2013].

The hygroscopicity of BC-containing aerosol has been measured directly in urban-impacted air masses with two different techniques: first by coupling a Hygroscopic Tandem Differential Mobility Analyzer with a single-particle soot photometer (SP2) [*Liu et al*., 2013; *McMeeking et al*., 2011] and second by sampling mass-selected dry aerosol with a humidified SP2 [*Ohata et al*., 2016]. Here we report measurements of BC hygroscopicity in wildfire plumes. Since 40% of the global BC burden is produced through open combustion [*Bond et al*., 2004], these measurements address a highly important BC source that has not been assessed in previous direct measurements of BC hygroscopicity. As described below, we use a humidified dual single-particle soot photometer (HD-SP2) [*Schwarz et al*., 2015], which compares dry and humidified measurements of BC-containing aerosol optical size made with two SP2s and report the observed differences using the hygroscopicity parameter, κ, introduced by *Petters and Kreidenweis* [2007].

2. Methods

2.1. Mission Description and Plume Selection Criteria

The SEAC^{4}RS mission took place during the summer of 2013, with the NASA DC-8 aircraft carrying the HD-SP2. An overview of the project has been published [*Toon et al*., 2016], and the data can be accessed publicly through DOI 10.5067/Aircraft/SEAC4RS/Aerosol-TraceGas-Cloud. Of the 21 total science flights, five included targeted sampling of wildfire plumes and are used in the present analysis. Two flights were dedicated exclusively to characterizing and studying the Yosemite Rim Fire in a semi-Lagrangian manner (i.e., the plume was traced downwind without staying with the same exact air parcel) as described previously [*Forrister et al*., 2015; *Saide et al*., 2015]. Wildfire plumes were identified by elevated acetonitrile concentrations (>200 pptv) as well as elevated carbon monoxide (CO) concentrations (available on four of five flights) and/or BC loadings relative to the surrounding air. Acetonitrile was measured using proton transfer mass spectrometry [*Wisthaler et al*., 2002], and CO was measured using the Differential Absorption CO measurement (DACOM) tunable diode laser instrument [*Sachse et al*., 1991, 1987]. A detailed discussion of the BC measurement technique can be found below. The semi-Lagrangian analysis of the Yosemite Rim Fire plume also incorporates observations of bulk aerosol composition, measured using a High-Resolution, Time of Flight, Aerosol Mass Spectrometer (HR ToF AMS, as described in detail in *DeCarlo et al*. [2006] and *Canagaratna et al*. [2007]). Several other measurements of aerosol hygroscopicity were also available, including ratios of bulk aerosol wet-to-dry scattering at 80%, $f(RH)_{80}$, using a humidified nephelometer [*Kotchenruther and Hobbs*, 1998; *Malm et al*., 2003] and size-resolved aerosol hygroscopicity measured by the Differential Aerosol Sizing and Hygroscopicity Spectrometer Probe (DASH-SP), as described by *Sorooshian et al*. [2008]. The latter instrument also provided size-resolved real refractive index data at a wavelength of 532 nm [*Shingler et al*., 2016a] assuming homogeneous spherical particles.

Using the selection criteria above, we identify a total of ~5 h of wildfire sampling during research flights that took place on 6, 16, 19, 26, and 27 August 2013. Single-particle BC data from individual plume crossings of less than 10 min in duration were integrated into a single data point, while plume samplings of longer than 10 min (primarily the Yosemite Rim Fire sampling) were analyzed to generate a series of 5 min samples. A total of 65 data points are thus generated, with a minimum integration time of 53 s and a maximum

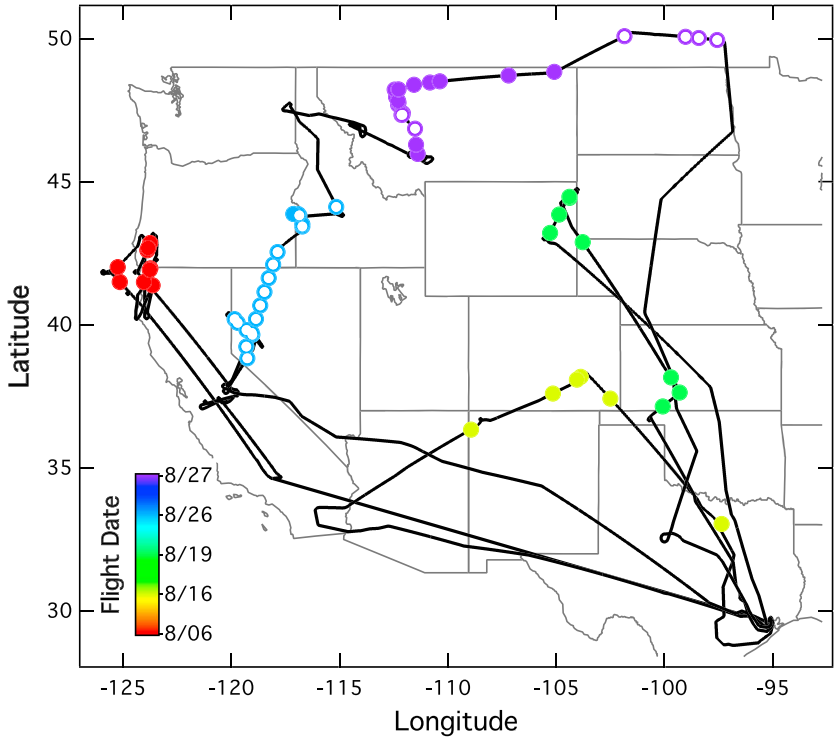

Figure 1. Map of five SEAC[4]RS flights with wildfire plume intercepts (black) with circles showing locations of individual plume sampling data points used in this analysis (colored by flight date). Open symbols indicate points for which back trajectories trace to the Yosemite Rim Fire.

integration time of 10 min. Of those, 25 data points have back trajectories tracing to the Yosemite Rim Fire specifically, while the remaining 40 arise from a variety of wildfires in the western U.S. and likely represent various fuels, burn conditions, and processing times. A map of the flight tracks and the locations of each averaged plume data point is shown in Figure 1. Data from a few plume crossings was omitted due to poor humidity control in the HD-SP2 (described in detail below) when the humidity of the sample and sheath flows disagreed by more than 2%.

2.2. BC Aerosol Methods

The single-particle soot photometer (SP2) is a laser-induced incandescence measurement for single-particle quantification of refractory BC mass, which has been described previously [*Schwarz et al.*, 2008]. Briefly, a high-intensity intracavity laser beam at 1064 nm results in heating of particles containing refractory BC to the BC incandescence temperature (~4000 K). These particles emit thermal radiation, the intensity of which is linearly proportional to the mass of BC contained in the particle. The sensitivity of the SP2 to single-particle BC mass was calibrated using size-selected Fullerene soot (Lot F12S011, Alfa Aesar Inc., Woodhill, MA), the accepted BC reference material for use with the SP2 [*Baumgardner et al.*, 2012], before, during, and after the mission and the instrument response was stable to within 5%. The SP2, as configured here, detects particles containing between 0.7 and 150 fg of refractory BC material (equivalent to core sizes of ~90 to 500 nm volume equivalent diameter assuming a void-free density of 1.8 g/cm^3) independent of the presence or amount of coexisting nonrefractory material.

The SP2 also provides optical sizing of individual BC-containing particles through analysis of elastically scattered laser light prior to significant thermal perturbation by the laser, as described by *Gao et al.* [2007]. A full recounting of the details of this technique is beyond the scope of this manuscript. Suffice it to say that this early scattering signal allows for quantification of nonrefractory material internally mixed with BC, which we refer to here generically as coatings. Coating thickness is calculated from the measured optical size using Mie theory, assuming a spherical core-shell morphology. *Ohata et al.* [2016] recently evaluated the accuracy of this method using mass-selected internal mixtures of laboratory aerosol. They found that the SP2

scattering estimate of coating thickness agreed with that calculated from the difference between the total particle mass and the BC core mass to within 10% for particles with a total diameter at least 1.5 times the diameter of the core (i.e., thickly coated particles). Although this study used idealized laboratory aerosol, the results indicate that coating thicknesses inferred from SP2-based measurements of optical size are reasonably related to actual coating thickness, especially for thickly coated particles. The assumed index of refraction for BC cores at 1064 nm (2.26, i1.26) is based on ambient BC measured in Tokyo [*Moteki and Kondo*, 2010] also consistent with observations of a variety of BC sources in Europe reported by *Laborde et al*. [2012]. The real refractive index assumed for (non-light-absorbing) coating material is 1.54, as reported for SEAC^{4}RS wildfire plumes by *Shingler et al*. [2016a], which was observed to vary by $\pm$0.02 over the course of an evolving plume. Scattering amplitudes in the SP2 were calibrated using 220 nm polystyrene-latex spheres, which were sampled prior to most flights. The detector gains used here provide optical sizing for particles from ~150 to 700 nm.

In the present study, two independent SP2s (one dry and one humidified) were operated in parallel, described further below, to examine water uptake by BC-containing particles. Both instruments subsampled isokinetically from an ambient aerosol stream collected by the NASA Langley aerosol inlet [*McNaughton et al*., 2007] that was dried immediately following aspiration. The total residence time from the tip of the inlet to detection by the SP2 was ~1 s. Transmission efficiency, calculated using equations from *Baron and Willeke* [2005], was high for submicron particles dropping to 50% transmission at 2 μm. Both SP2s were run under identical (dry) conditions with no humidification during test flights, and the level of agreement was assessed for BC mass distributions (mass median diameters matched to within 2 nm), BC mass mixing ratios (within 5%), and observed scattering (within 5% in log space) from selected BC core mass ranges (typically a 2 fg "slice" between 3 and 10 fg). BC data were excluded under high aerosol number concentrations (whenever the incidence of coincident particles in the SP2 exceeded a few percent, a function of sample flow, typically occurring when loadings were above about 1000/cm^3) because data quality is significantly reduced and retrieval of optical particle sizes needed for this analysis are not possible. Data were also excluded during periods of cloud sampling (identified from a combination of forward camera video feeds and observational evidence of cloud artifacts in aerosol instrumentation) due to known artifacts that arise from impaction of both liquid droplets and ice particles on inlet surfaces [*Perring et al*., 2013].

2.3. Measurement of BC-Containing Aerosol Hygroscopicity

The use of two SP2s operating in parallel (the Humidified Dual-SP2 or HD-SP2) allows us to examine water uptake by BC-containing particles on a population basis. During science flights, one SP2 sampled the dried ambient aerosol stream (the "dry SP2") while the other humidified the dried sample stream to a stable relative humidity (typically 90%) prior to measurement (the "wet SP2"). The hygroscopicity of materials internally mixed with BC (BC coatings) is reported in terms of κ, a unitless parameter introduced by *Petters and Kreidenweis* [2007], which relates the dry volume of a material to the volume of water that will be taken up by that material at a given humidity. κ values for atmospheric aerosol range from 0 for nonhygroscopic materials (e.g., bare black carbon and some organics) to $>$1 for highly hygroscopic materials such as H_2SO_4 or HNO_3.

Full details of the humidification strategy and data analysis methodology used in the HD-SP2 are provided in *Schwarz et al*. [2015]. Briefly, we first select a size range of BC "cores" for which both instruments reported an optical size for nearly all BC-containing particles. At small BC core sizes, scattering signals off thinly coated cores are too small to allow retrieval of the total particle optical size; hence, those optical sizes are only retrieved for thickly coated cores, leading to potential analytical bias. At larger core sizes the number concentrations decrease, leading to reduced statistics. Therefore, it is preferable to analyze particles with the smallest BC cores for which we have good optical sizing over the full range of coating thicknesses; here the size range chosen is 4–6 fg (~160–185 nm volume equivalent diameter or VED), near the center of the accumulation mode BC mass distribution for the plumes examined here (shown in Figure S1 in the supporting information). The modal scattering for this selected range of BC masses in the dry instrument is used to calculate the dry coating thickness. The dry coating thickness is then used to calculate theoretical scattering amplitudes at the RH of the wet SP2 for a range of κ (including adjustment of the coating refractive index to account for water uptake), and the reported κ value is that for which the observed wet modal scattering best matches the theoretical wet scattering. Statistical error in individual particle mass determinations (of order

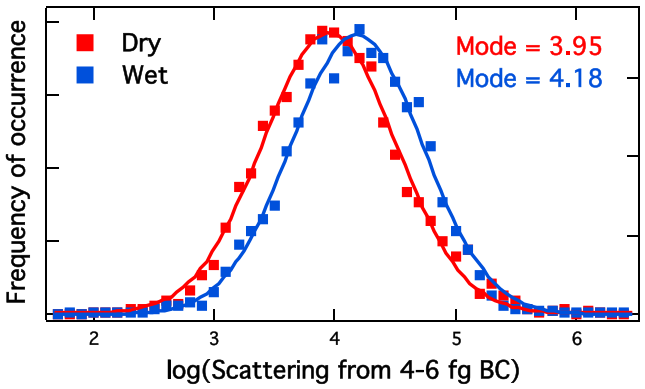

Figure 2. Example of modal scattering from selected BC core sizes in the wet and dry SP2s from the flight of 6 August 2013. This wet-to-dry difference represents a BC-specific κ value of 0.08.

10%) broadens the modal scattering distributions slightly but does not change the center of the distribution and is therefore neglected. Further details regarding the full treatment of the theoretical scattering amplitude calculation as well as a discussion regarding the use of "modal" scattering as opposed to "average" scattering can be found in *Schwarz et al*. [2015].

To allow for situations where light scattering observed in the wet SP2 was less than in the dry system (most likely due to statistical uncertainties but potentially also from phenomena not accounted for in the approach outlined above such as core collapse), the range of κ used in the optimization extends below zero (i.e., into a range not associated with physical meaning in the Petters and Kreidenweis model). In this case (which occurred in $<$20% of the plumes discussed here), the scattering signals of the dry and wet SP2s were simply swapped in the optimization such that a kappa value was calculated as if the humidified distribution had "grown" into the dry distribution and that value is reported as a negative.

Schwarz et al. [2015] use theoretical calculations to assess the uncertainty associated with κ values reported for BC coating materials using the HD-SP2 technique. They find that shifting the assumed density of the BC core by 20% (a 6% shift in the BC core diameter) covering one third of the range of BC density estimates presented in *Moteki and Kondo* [2010] results in an 11% shift in the derived κ value. Similarly, shifting the assumed refractive index of the coating by about one third of the range of expected atmospheric coating indices results in a 17% shift in κ. Finally, they find a 22% uncertainty in κ arising from uncertainties in the performance of the theoretical treatment. Summing these uncertainties in quadrature, they report an overall uncertainty of 30% in κ for BC with thick coatings. Conceptually, it is logical that the uncertainty in κ for materials associated with BC is inversely proportional to the coating thickness because, as coatings become thicker, the BC component is responsible for a smaller fraction of the total particle scatter and the optical behavior of the particle approaches that of a homogeneous material. A graphical representation of this behavior is shown in Figure 4 of *Schwarz et al*. [2015] which provides a contour plot of wet to dry scattering ratio as a function of coating thickness and κ. For coatings above 40 nm, a given wet to dry scattering ratio provides a very strong constraint on κ with little dependence on the exact coating thickness, especially for $\kappa < 0.2$.

In the present work, a larger uncertainty in derived κ arises from the cross calibration of scattering amplitudes in the two SP2s which is critical for proper interpretation of wet-to-dry scatter ratio values. Drift in the relative scattering between the two instruments arises in flight from independent variations in laser power. Thus, it was necessary to apply a small ($<$5%) adjustment to the wet SP2 scattering, assessed on a flight-by-flight basis in addition to scaling each SP2 according to PSLs in preflight. This adjustment was based on in-flight observations by matching modal scattering from bare BC cores of a given mass in the wet instrument to that observed in the dry SP2 when sampling fresh BC with no evidence of coatings, expected to have minimal hygroscopic growth. Using scattering amplitudes associated with BC cores, after coatings have been removed and just prior to incandescence (the core scattering), we find that the single-flight standard deviation of the wet to dry ratio of modal core scattering from 4 to 6 fg BC particles was less than 2.5% for all flights, and we take this value as our uncertainty in the wet scattering scale factor. A 2.5% cross-calibration uncertainty corresponds to a κ uncertainty of 0.04.

Figure 2 shows an example of scattering amplitude distributions observed for 4–6 fg BC cores in the wet (shown in blue) and dry (shown in red) SP2s, from the flight on 6 August, with modal values identified. Modal scattering is calculated in log space due to the exponential relationship between particle size and elastic scattering and to reduce the impact of spurious signals. Although little water uptake is observed

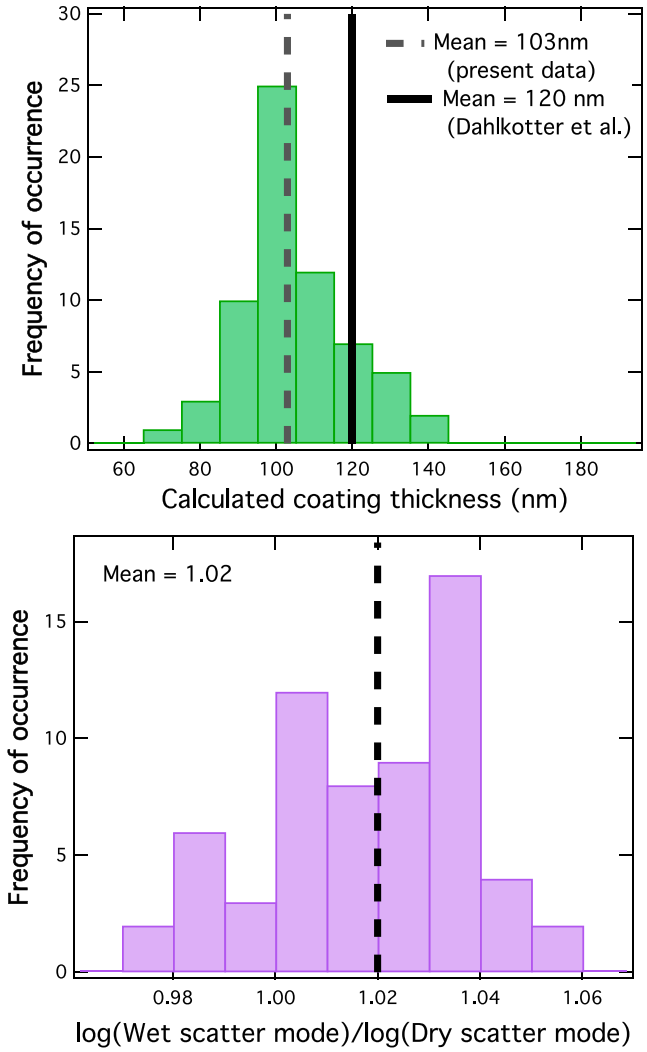

Figure 3. (top) Histogram of observed dry coating thicknesses for 4–6 fg BC cores in all biomass burning plumes sampled and (bottom) histogram of the observed ratio of log(wet) to log(dry) modal scattering from 4 to 6 fg BC cores at 90% RH.

(the calculated κ value for this plume is 0.08), this amount of signal is larger than the uncertainty in cross calibrating the scattering in the wet and dry SP2.

3. Results and Discussion

3.1. Aggregate Observations of All Identified Plumes

Figure 3 (top) shows a histogram of dry coating thicknesses observed for 4–6 fg BC cores in all wildfire plumes (of all ages) identified in this work. The wildfire BC was uniformly thickly coated, and the variability in coating thickness between different plumes sampled was relatively small. These particles are 10% BC and 90% coating on a volume basis and ~16% BC and 84% coating on a mass basis (assuming void-free densities of 1.8 g/cm^3 and 1 g/cm^3 for BC and coatings, respectively). For comparison we show the mean coating thickness reported by *Dahlkötter et al.* [2014] (~120 nm on 2.5 to 4 fg) for a very aged plume from the Pagami Creek Fire, which was measured over the North Atlantic Ocean in 2012. Most of this difference is attributable to different assumed refractive indices for the coating. Here we assume a real index of refraction for the coatings of 1.54 as reported by *Shingler et al.* [2016a]. If we, instead, assume the index (1.45) used by *Dahlkötter et al.* [2014], we would have a mean coating thickness of 115 nm. This is a striking agreement in coating thickness measured for different wildfire plumes of different ages by different SP2s and is in general agreement with shell/core ratios reported by *Kondo et al.* [2011] for North American and Asian biomass burning plumes. Thus, we see general consistency of BC produced from wildfire in terms of the presence and amount of internally mixed nonrefractory material after initial aging over the first few hours as described by *Akagi et al.* [2012]. Coating thickness was also examined over a range of BC core masses (shown in Figure S1), and little variation is seen, at least over the BC mass range from 150 to 260 nm VED for which we can retrieve modal coating thicknesses with good statistics.

Figure 3 (bottom) shows a histogram of the observed ratio of wet-to-dry modal scattering when the wet SP2 was sampled at 90% RH (functionally equivalent to f(RH)$_{90}$ measured at 1064 nm). The mean ratio is 1.02, indicating little water uptake by wildfire BC in aggregate, in general agreement with *Shingler et al.* [2016b] who report little water uptake for size-selected bulk biomass burning aerosol during SEAC^{4}RS. *Martin et al.* [2013] reported collapse of fractal carbon aggregates in fresh emissions from several combustion sources upon humidification, which would result in a reduction in scattering following humidification. We see little evidence of collapse in the present data set, which we hypothesize to mean that truly "fresh" emissions (minutes of aging) were never sampled due to restrictions imposed by aircraft operations such that any

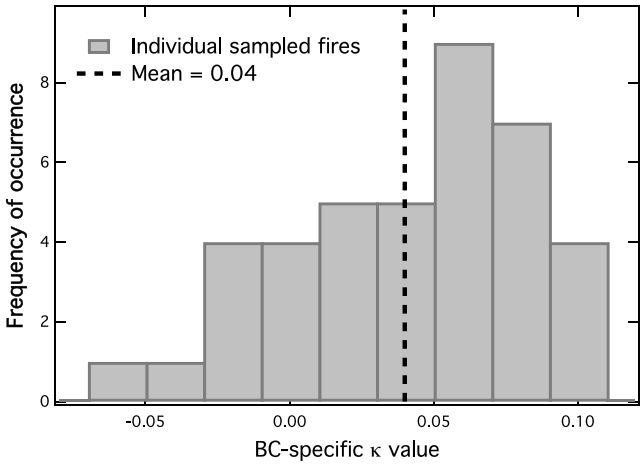

Figure 4. Histogram of BC-specific κ values calculated from the wet-to-dry modal scattering ratio for a semistatistical sampling of biomass burning plumes (excluding the Yosemite Rim Fire).

restructuring had already occurred prior to sampling. This hypothesis is supported by the ubiquity of thick coatings in this data set, which is in contrast with laboratory studies of freshly produced biomass burning aerosol. It is possible that restructuring is still occurring and is masked by water uptake, which would introduce a bias to our reported scattering ratios.

Figure 4 shows a histogram of the calculated κ values for the ensemble of wildfire plumes sampled, with the exception of the Yosemite Rim Fire, which is discussed in more detail below. This ensemble represents only the plumes sampled during the SEAC^{4}RS study and certainly represents various burn conditions and atmospheric ages. The observed κ values are low (ensemble average value = 0.04 $\pm$ 0.04), typical of less oxidized organic material and in general agreement with κ values reported previously in the size range studied here for bulk biomass burning aerosol in laboratory settings [*Dusek et al*., 2011; *Martin et al*., 2013; *Petters et al*., 2009; *Wonaschuetz et al*., 2013] and field observations [*Lathem et al*., 2013; *Wonaschuetz et al*., 2013]. We see little variation in κ as a function of particle size over the range of BC core sizes for which we can extract hygroscopicity information (2–12 fg or 130–230 nm VED, shown in Figure S1). Several studies [*Martin et al*., 2013; *Petters et al*., 2009] have reported a more hygroscopic mode at particle sizes $<$100 nm; however, the present results cannot speak to this finding as we are only effectively probing total particle sizes from 350 to 500 nm diameter, a much more restricted range than examined previously for bulk aerosol.

As stated in *Schwarz et al*. [2015], the uncertainty in κ determined with the HD-SP2 system is typically dominated by uncertainty in the dry coating thickness and the refractive index of the coating, with larger uncertainties associated with larger κ values. For plumes presented here, which had uniformly thick coatings, low hygroscopic growth, and for which we have a reasonable estimate of the real part of the coating refractive index, these uncertainties are relatively small and the uncertainty in κ is, instead, dominated by our ability to accurately relate scattering amplitudes in the wet instrument to that in the dry. As discussed above, this uncertainty is assessed at $\pm$2.5%, corresponding to an uncertainty in κ of ~($\pm$0.04).

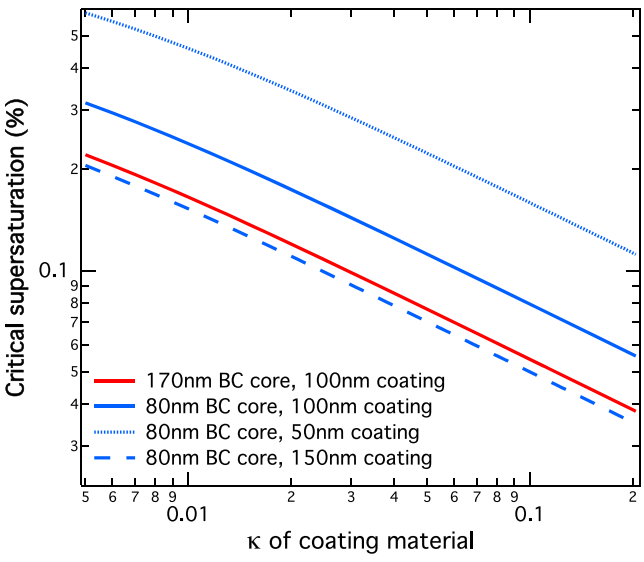

Figure 5. Calculated critical supersaturation for different BC core sizes and coating thicknesses as a function of the coating material κ.

When considering water uptake by aerosol, it is also useful to examine the critical supersaturation, defined as the minimum supersaturation (*s*), with respect to water, at which a particle will fail to equilibrate, instead growing without limit and thus serving as an effective cloud condensation nucleus (CCN). Using equation 6 from *Petters and Kreidenweis* [2007] and following the treatment in *McMeeking et al*. [2011], we have calculated critical supersaturations, for representative wildfire-generated BC particles as a function of the κ of the coating material (shown in Figure 5). Calculations were performed

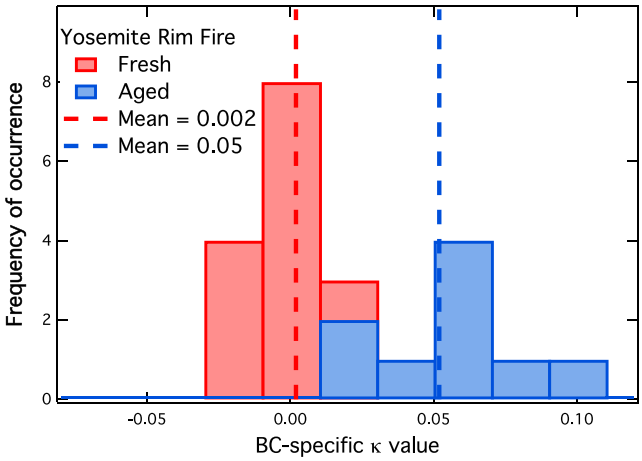

Figure 6. Histogram of BC-specific κ values observed in the Yosemite Rim Fire plume. Red shows plume samplings with an estimated age <24 h, blue shows those with an estimated age >24 h, and dotted lines show the mean value of the two populations.

for 170 nm BC cores (near the center of the wildfire BC mass distribution) with the observed 100 nm of coating and for 80 nm BC cores (near the center of the wildfire BC number distribution) with 50, 100, and 150 nm coating thickness.

For a 170 nm BC core with 100 nm coating thickness, the particle is an active CCN at a supersaturation of 0.2% (a commonly used threshold for CCN activity) if the κ of the coating material is higher than 0.007. Thus, the majority of the accumulation mode BC mass was contained in particles that were CCN active at $s = 0.2\%$ in 85% of the plumes sampled here. For an 80 nm core, the minimum coating material κ required to activate at 0.2% supersaturation is 0.005, 0.02, and 0.08 for 150, 100, and 50 nm coating thicknesses, respectively. Thus, most of the accumulation mode BC number was contained in particles that were CCN active at $s = 0.2\%$ in most plumes (70% for the 100 nm case and 85% for the 150 nm case) if smaller BC is at least as thickly coated as larger BC. This finding is largely due to the presence of thick coatings on BC cores, which increases the total particle size substantially, bringing most of the BC-containing particles into a size range where they act as efficient CCN even though they are not very hygroscopic. Results presented here are in broad agreement with observations reported by *Hersey et al*. [2013] for a biomass burning plume sampled during the CalNex study of 2010 and likely indicates that biomass burning BC will be removed relatively efficiently via wet processing.

3.2. Temporal Evolution Observed in the Yosemite Rim Fire

The flights of 26 and 27 August were focused on tracking the Yosemite Rim Fire downwind from the source in a semi-Lagrangian manner and have been described in several recent manuscripts [*Forrister et al*., 2015; *Saide et al*., 2015]. We sampled air that was emitted over the course of 2 days, and we assume that the available fuel and the large-scale burn conditions were not highly variable over that time. Back trajectories were run for each wildfire data point using the NOAA Hybrid Single-Particle Lagrangian Integrated Trajectory model [*Draxier and Hess*, 1998; *Stein et al*., 2015] with the North American Regional Reanalysis. Transport times were extracted for all trajectories that passed within 160 km of the Rim Fire extent. Data points were excluded from the aging analysis if back trajectories indicated passage near another significant fire or if in situ data indicated a substantially different plume composition (typically indicated by acetonitrile concentrations, extent of OA oxidation as indicated by the AMS and/or dramatic shifts in BC microphysical tracer properties). As discussed in *Forrister et al*. [2015], back trajectories for the 8/27 flight are somewhat ambiguous as to whether they are most recently impacted by the Yosemite Rim Fire or the Elk Creek Complex fire. Chemical tracers indicate similar plume composition between the end of the 8/26 flight and the beginning of the 8/27 flight; however, it is possible that the 8/27 flight sampled a mixture of the two fires. In the Forrister work the authors calculate back trajectories to both fires and present chemical evolution for both sets of ages in parallel. Here for simplicity, we present back trajectory ages to the Yosemite Rim Fire (which span plume ages from 1 to ~40 h) with the understanding that there may have been some more recent injections of fresh smoke. Note that due to data quality issues arising under extremely high particle loads, the earliest estimated time for which we were able to extract BC hygroscopicity information is ~4 h from the time of emission.

Figure 6 shows histograms of κ values observed in the Rim Fire for fresh (indicating a back trajectory age of <=24 h) and "aged" (indicating a time since emission of >24 h). These two histograms demonstrate the effects of atmospheric processing on observed BC-specific κ values with κ increasing over time. Note that the range of observed κ values in the Yosemite Rim Fire plume is similar to the range observed for our pseudo

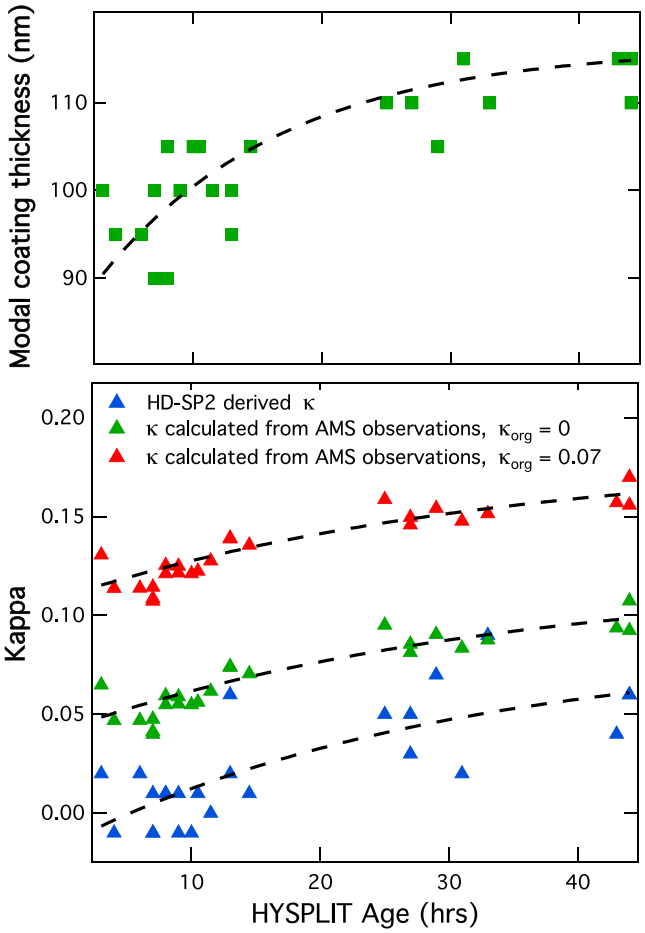

Figure 7. Temporal evolution in the Yosemite Rim Fire plume of (top) coating thickness on 4–6 fg BC cores and (bottom) BC-specific κ values calculated for 4–6 fg BC cores (blue) and κ values calculated for bulk aerosol based on AMS measurements assuming $\kappa = 0$ for organic materials (in green) and assuming $\kappa = 0.07$ for organic materials (in red). Dashed lines show exponential fits to the data.

statistical sampling of various wildfires presented above, indicating that different aging processes occurring after the first hours and through the first few days since emission can account for most of the observed variability between plumes. It also indicates that for the set of plumes studied here, variability in BC-containing aerosol κ values resulting from different fuel types and burn conditions was no larger than that introduced by atmospheric processing.

The potential aging pathways for BC-containing aerosol in wildfire plumes include evaporation of primary organic aerosol, direct or postoxidation deposition of inorganic and organic species from the gas phase, chemical processing of existing coating materials in the particle phase, and coagulation with other aerosol particles that may be aging simultaneously. Figure 7 (top) shows the temporal evolution of coating thickness as a function of estimated time since emission. Although the variability of coating thickness in the various biomass burning plumes sampled is small compared to the variability between biomass burning BC and other sources, there is a detectable upward trend in coating thickness with time since emission, at least over the first 2 days of aging. The observed coating thickness increase is ~20 nm in 40 h (corresponding to a 35% increase in total particle volume). This increase suggests that a combination of coagulation and continued deposition of inorganic and organic gas phase precursors presents in biomass burning plumes as they are oxidized to less volatile daughter products, as well as transfer of semivolatile species via the gas phase [*Marcolli et al.*, 2004], exceeded evaporation induced by dilution. We note that this finding does not contradict studies which find a lack of net secondary organic aerosol formation for most BB plumes [*Cubison et al.*, 2011; *Forrister et al.*, 2015; *Jolleys et al.*, 2012], since BC-containing particles are only a small percentage of the total particle population. An increase in the calculated BC-specific κ value (shown in Figure 7, bottom) is also observed with increasing plume age, corresponding to a κ increase of 0.06 over 40 h. The trends in both coating thickness and BC-specific κ are fit well with simple exponential curves. Though small changes in refractive index ($\pm$0.02) were observed by DASH-SP over the plume evolution, these shifts are too small to substantially affect the reported trends in either calculated coating thickness or, in turn, BC-specific kappa value.

Shown for comparison are calculated κ values for the bulk aerosol based on reported AMS mass fractions using the Zdanovskii-Stokes-Robinson mixing rule [*Petters and Kreidenweis*, 2007]. This comparison is potentially informative as to the chemical mechanism driving the observed change in κ. The bulk aerosol mass fractions of the ionic species used in this calculation are shown in Figure 8 (top), and the balance was organic aerosol mass. Ammonium balanced sulfate and nitrate on a molar basis at all times (sometimes with a slight excess of ammonium that can be explained by the presence of small concentrations of organic acid salts), so we assume that all of the NO_3 is present in the form of ammonium nitrate (NH_4NO_3) and all of the SO_4 is

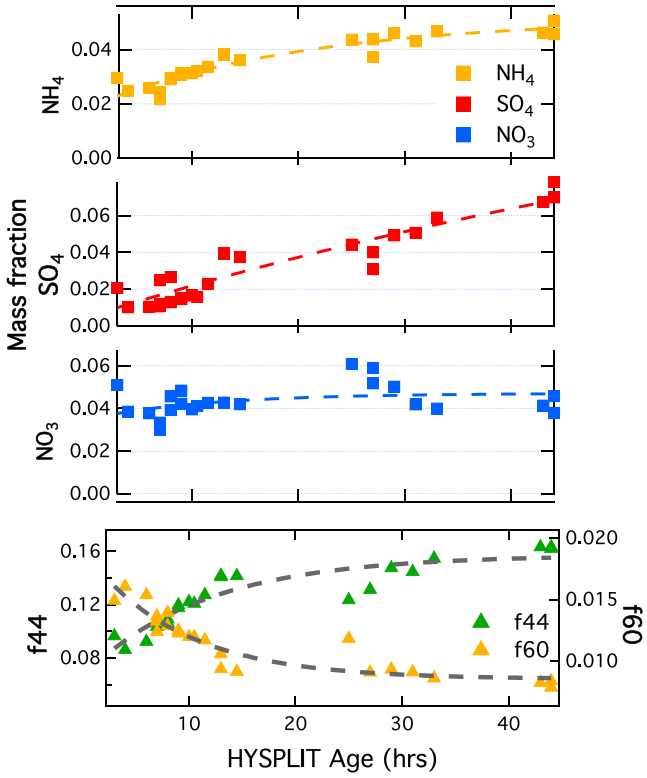

Figure 8. Temporal evolution in the Yosemite Rim Fire plume of (top) the AMS SO_4 (red), NH_4 (orange), and NO_3 (blue) mass fractions and (bottom) the AMS f44 (green) and f60 (yellow) atomic ratios of OA.

present in the form of ammonium sulfate ($[NH_4]_2SO_4$) which have reported κ values of 0.57 and 0.53, respectively. Reported κ values for organic aerosol components vary from 0.006 to 0.165 [*Rickards et al.*, 2013; *Suda et al.*, 2014]. Here we first assume $\kappa = 0$ for organics such that the calculated bulk aerosol hygroscopicity shown is the minimum possible bulk aerosol κ value. The trend in calculated bulk κ is offset from but shows a similar net increase to that observed by the HD-SP2 for BC-containing aerosol. The magnitude of the offset is 0.04 assuming an organic κ of 0, the minimum possible calculated bulk κ. If, instead, we assume an organic κ of 0.07 as reported by *Shingler et al.* [2016a], which falls in the middle of the published range, the offset increases to 0.12. This offset is likely sufficiently large to imply initial differences in chemical composition between bulk aerosol and materials internally mixed with BC (again, a minor fraction of total particles) in biomass burning plumes.

The magnitude of the increase in κ values, on the other hand, is remarkably similar between bulk aerosol and BC-containing aerosol (0.055 and 0.065 respectively over the plume ages sampled), consistent with similar processing mechanisms for the two populations, regardless of the organic κ value assumed. In the bulk aerosol, we see that NO_3 is the dominant ionic component by mass early in the plume but does not change substantially over time. The observed increases in NH_4 and SO_4 are roughly in molar balance and are equivalent to an 8% increase in the mass fraction of ammonium sulfate over the plume ages studied. All other things being equal, this incorporation of ammonium sulfate would lead to an increase of 0.042 in the bulk aerosol κ, which explains approximately two thirds of the observed κ increase in both bulk aerosol and BC-containing particles. Figure 8 (bottom) shows the temporal evolution of the H:C and O:C ratios reported by the AMS, which indicate the level of oxidation of the bulk aerosol. More oxidized organic aerosol is known to be generally more hygroscopic [*Chang et al.*, 2010; *Jimenez et al.*, 2009; *Lambe et al.*, 2013; *Suda et al.*, 2014] which likely explains the remainder of the observed increase in κ values for both the bulk aerosol and for BC-containing particles. The observed BC-specific κ value increase is fit well with a simple exponential curve corresponding to a transition from an initial κ of 0 to a final κ of 0.09 with an *e*-folding time of 29 h.

4. Conclusions

Water uptake by BC-containing aerosol has been quantified in wildfire plumes detected over the continental U.S. during the summer of 2013. We find that wildfire-generated BC is uniformly thickly coated and only weakly hygroscopic with an ensemble average BC-specific κ value of 0.04 ($\pm$0.04) over the wildfire plumes sampled. Calculations indicate that for the vast majority (85%) of these plumes, most of the mass of BC emitted is CCN active at 0.2% supersaturation. The Yosemite Rim Fire was tracked in a semi-Lagrangian manner for plume ages spanning from 1 to 40 h. Over that time, BC coating thickness is observed to increase slightly (from 90 nm to 110 nm for 4–6 fg BC cores) and the BC-specific κ value increases by 0.06. A similar increase in κ is calculated from AMS measurements of aerosol composition, likely indicating similar chemical evolution between the two populations. Using observed changes in aerosol composition, we attribute two thirds of the observed κ increase to incorporation of ammonium sulfate and we hypothesize that the balance

of the increase is driven by increased oxidation of organic aerosol components and/or incorporation of oxidized organics from the gas phase. These findings provide unique, direct constraints on the behavior and evolution of BC-containing aerosol arising from wildfire plumes, a globally important source of BC aerosol, which improve our mechanistic understanding of the processes governing the lifetime and removal of BC aerosol in the atmosphere.

Acknowledgments
All data for the SEAC4RS project are publicly available at DOI 10.5067/Aircraft/SEAC4RS/Aerosol-TraceGas-Cloud. NOAA SP2 research conducted by A.P., M.M., J.S., R.S.G., and D.F. was supported by the NOAA Atmospheric Composition and Climate Program, the NASA Radiation Sciences Program, and the NASA Upper Atmosphere Research Program. A.S. and T.S. were funded by NASA grants NNX12AC10G, NNX14AP75G, and NNX14AK79H. P.C.J., B.D.P., and J.L.J. were supported by NASA grants NNX12AC03G and NNX15AT96G. R.Y. was supported by NASA Earth Science Division Awards NNX12AC20G and NNX14AP45G.

References

Akagi, S. K., et al. (2012), Evolution of trace gases and particles emitted by a chaparral fire in California, *Atmos. Chem. Phys.*, *12*(3), 1397–1421, doi:10.5194/acp-12-1397-2012.

Baron, P. A., and K. Willeke (2005), *Aerosol Measurement: Principles, Techniques and Applications*, Van Nostrond Reinhold, New York.

Baumgardner, D., et al. (2012), Soot reference materials for instrument calibration and intercomparisons: A workshop summary with recommendations, *Atmos. Meas. Tech.*, *5*(8), 1869–1887, doi:10.5194/amt-5-1869-2012.

Bond, T. C., D. G. Streets, K. F. Yarber, S. M. Nelson, J. H. Woo, and Z. Klimont (2004), A technology-based global inventory of black and organic carbon emissions from combustion, *J. Geophys. Res. Atmos.*, *109*, D14203, doi:10.1029/2003JD003697.

Bond, T. C., et al. (2013), Bounding the role of black carbon in the climate system: A scientific assessment, *J. Geophys. Res. Atmos.*, *118*, 5380–5552, doi:10.1002/jgrd.50171.

Canagaratna, M. R., et al. (2007), Chemical and microphysical characterization of ambient aerosols with the aerodyne aerosol mass spectrometer, *Mass Spec. Rev.*, *26*(2), 185–222, doi:10.1002/mas.20115.

Cape, J. N., M. Coyle, and P. Dumitrean (2012), The atmospheric lifetime of black carbon, *Atmos. Environ.*, *59*, 256–263, doi:10.1016/j.atmosenv.2012.05.030.

Chang, R. Y. W., J. G. Slowik, N. C. Shantz, A. Vlasenko, J. Liggio, S. J. Sjostedt, W. R. Leaitch, and J. P. D. Abbatt (2010), The hygroscopicity parameter (kappa) of ambient organic aerosol at a field site subject to biogenic and anthropogenic influences: Relationship to degree of aerosol oxidation, *Atmos. Chem. Phys.*, *10*(11), 5047–5064, doi:10.5194/acp-10-5047-2010.

Chung, S. H., and J. H. Seinfeld (2002), Global distribution and climate forcing of carbonaceous aerosols, *J. Geophys. Res.*, *107*(D19), 4407, doi:10.1029/2001JD001397.

Cooke, W. F., and J. J. N. Wilson (1996), A global black carbon aerosol model, *J. Geophys. Res.*, *101*(D14), 19,395–19,409, doi:10.1029/96JD00671.

Cubison, M. J., et al. (2011), Effects of aging on organic aerosol from open biomass burning smoke in aircraft and laboratory studies, *Atmos. Chem. Phys.*, *11*(23), 12,049–12,064, doi:10.5194/acp-11-12049-2011.

Dahlkötter, F., M. Gysel, D. Sauer, A. Minikin, R. Baumann, P. Seifert, A. Ansmann, M. Fromm, C. Voigt, and B. Weinzierl (2014), The Pagami Creek smoke plume after long-range transport to the upper troposphere over Europe—Aerosol properties and black carbon mixing state, *Atmos. Chem. Phys.*, *14*(12), 6111–6137, doi:10.5194/acp-14-6111-2014.

DeCarlo, P. F., et al. (2006), Field-deployable, high-resolution, time-of-flight aerosol mass spectrometer, *Anal. Chem.*, *78*(24), 8281–8289, doi:10.1021/ac061249n.

Draxier, R. R., and G. D. Hess (1998), An overview of the HYSPLIT_4 modelling system for trajectories, dispersion and deposition, *Aust. Meteorol. Mag.*, *47*(4), 295–308.

Dusek, U., G. P. Reischl, and R. Hitzenberger (2006), CCN activation of pure and coated carbon black particles, *Environ. Sci. Technol.*, *40*(4), 1223–1230, doi:10.1021/es0503478.

Dusek, U., G. P. Frank, A. Massling, K. Zeromskiene, Y. Iinuma, O. Schmid, G. Helas, T. Hennig, A. Wiedensohler, and M. O. Andreae (2011), Water uptake by biomass burning aerosol at sub- and supersaturated conditions: Closure studies and implications for the role of organics, *Atmos. Chem. Phys.*, *11*(18), 9519–9532, doi:10.5194/acp-11-9519-2011.

Forrister, H., et al. (2015), Evolution of brown carbon in wildfire plumes, *Geophys. Res. Lett.*, *42*, 4623–4630, doi:10.1002/2015GL063897.

Gao, R. S., et al. (2007), A novel method for estimating light-scattering properties of soot aerosols using a modified single-particle soot photometer, *Aerosol Sci. Technol.*, *41*(2), 125–135, doi:10.1080/02786820601118398.

Hersey, S. P., et al. (2013), Composition and hygroscopicity of the Los Angeles Aerosol: CalNex, *J. Geophys. Res. Atmos.*, *118*, 3016–3036, doi:10.1002/jgrd.50307.

Jimenez, J. L., et al. (2009), Evolution of organic aerosols in the atmosphere, *Science*, *326*(5959), 1525–1529, doi:10.1126/science.1180353.

Jolleys, M. D., et al. (2012), Characterizing the aging of biomass burning organic aerosol by use of mixing ratios: A meta-analysis of four regions, *Environ. Sci. Technol.*, *46*(24), 13,093–13,102, doi:10.1021/es302386v.

Koehler, K. A., P. J. DeMott, S. M. Kreidenweis, O. B. Popovicheva, M. D. Petters, C. M. Carrico, E. D. Kireeva, T. D. Khokhlova, and N. K. Shonija (2009), Cloud condensation nuclei and ice nucleation activity of hydrophobic and hydrophilic soot particles, *Phys. Chem. Chem. Phys.*, *11*(36), 7906–7920, doi:10.1039/b905334b.

Kondo, Y., et al. (2011), Emissions of black carbon, organic, and inorganic aerosols from biomass burning in North America and Asia in 2008, *J. Geophys. Res.*, *116*, D08204, doi:10.1029/2010JD015152.

Kotchenruther, R. A., and P. V. Hobbs (1998), Humidification factors of aerosols from biomass burning in Brazil, *J. Geophys. Res.*, *103*(D24), 32,081–32,089, doi:10.1029/98JD00340.

Laborde, M., et al. (2012), Single Particle Soot Photometer intercomparison at the AIDA chamber, *Atmos. Meas. Tech.*, *5*(12), 3077–3097, doi:10.5194/amt-5-3077-2012.

Lambe, A. T., et al. (2013), Relationship between oxidation level and optical properties of secondary organic aerosol, *Environ. Sci. Technol.*, *47*(12), 6349–6357, doi:10.1021/es401043j.

Lathem, T. L., A. J. Beyersdorf, K. L. Thornhill, E. L. Winstead, M. J. Cubison, A. Hecobian, J. L. Jimenez, R. J. Weber, B. E. Anderson, and A. Nenes (2013), Analysis of CCN activity of Arctic aerosol and Canadian biomass burning during summer 2008, *Atmos. Chem. Phys.*, *13*(5), 2735–2756, doi:10.5194/acp-13-2735-2013.

Liu, D., J. Allan, J. Whitehead, D. Young, M. Flynn, H. Coe, G. McFiggans, Z. L. Fleming, and B. Bandy (2013), Ambient black carbon particle hygroscopic properties controlled by mixing state and composition, *Atmos. Chem. Phys.*, *13*(4), 2015–2029, doi:10.5194/acp-13-2015-2013.

Malm, W. C., D. E. Day, S. M. Kreidenweis, J. L. Collett, and T. Lee (2003), Humidity-dependent optical properties of fine particles during the Big Bend regional aerosol and visibility observational study, *J. Geophys. Res.*, *108*(D9), 4279, doi:10.1029/2002JD002998.

Marcolli, C., B. P. Luo, and T. Peter (2004), Mixing of the organic aerosol fractions: Liquids as the thermodynamically stable phases, *J. Phys. Chem. A*, *108*(12), 2216–2224, doi:10.1021/jp036080l.

Martin, M., et al. (2013), Hygroscopic properties of fresh and aged wood burning particles, *J. Aerosol Sci.*, *56*, 15–29, doi:10.1016/j.jaerosci.2012.08.006.
McMeeking, G. R., N. Good, M. D. Petters, G. McFiggans, and H. Coe (2011), Influences on the fraction of hydrophobic and hydrophilic black carbon in the atmosphere, *Atmos. Chem. Phys.*, *11*(10), 5099–5112, doi:10.5194/acp-11-5099-2011.
McNaughton, C. S., et al. (2007), Results from the DC-8 Inlet Characterization Experiment (DICE): Airborne versus surface sampling of mineral dust and sea salt aerosols, *Aerosol Sci. Technol.*, *41*(2), 136–159, doi:10.1080/02786820601118406.
Moffet, R. C., and K. A. Prather (2009), In-situ measurements of the mixing state and optical properties of soot with implications for radiative forcing estimates, *Proc. Natl. Acad. Sci. U.S.A.*, *106*(29), 11,872–11,877, doi:10.1073/pnas.0900040106.
Moteki, N., and Y. Kondo (2010), Dependence of laser-induced incandescence on physical properties of black carbon aerosols: Measurements and theoretical interpretation, *Aerosol Sci. Technol.*, *44*(8), 663–675, doi:10.1080/02786826.2010.484450.
Moteki, N., Y. Kondo, N. Oshima, N. Takegawa, M. Koike, K. Kita, H. Matsui, and M. Kajino (2012), Size dependence of wet removal of black carbon aerosols during transport from the boundary layer to the free troposphere, *Geophys. Res. Lett.*, *39*, L13802, doi:10.1029/2012GL052034.
Ohata, S., J. P. Schwarz, N. Moteki, M. Koike, A. Takami, and Y. Kondo (2016), Hygroscopicity of materials internally mixed with black carbon measured in Tokyo, *J. Geophys. Res. Atmos.*, *121*, 362–381, doi:10.1002/2015JD024153.
Perring, A. E., J. P. Schwarz, R. S. Gao, A. J. Heymsfield, C. G. Schmitt, M. Schnaiter, and D. W. Fahey (2013), Evaluation of a perpendicular inlet for airborne sampling of interstitial submicron black-carbon aerosol, *Aerosol Sci. Technol.*, *47*(10), 1066–1072, doi:10.1080/02786826.2013.821196.
Petters, M. D., and S. M. Kreidenweis (2007), A single parameter representation of hygroscopic growth and cloud condensation nucleus activity, *Atmos. Chem. Phys.*, *7*(8), 1961–1971.
Petters, M. D., A. J. Prenni, S. M. Kreidenweis, P. J. DeMott, A. Matsunaga, Y. B. Lim, and P. J. Ziemann (2006), Chemical aging and the hydrophobic-to-hydrophilic conversion of carbonaceous aerosol, *Geophys. Res. Lett.*, *33*, L24806, doi:10.1029/2006GL027249.
Petters, M. D., C. M. Carrico, S. M. Kreidenweis, A. J. Prenni, P. J. DeMott, J. L. Collett Jr., and H. Moosmueller (2009), Cloud condensation nucleation activity of biomass burning aerosol, *J. Geophys. Res.*, *114*, D22205, doi:10.1029/2009JD012353.
Rickards, A. M. J., R. E. H. Miles, J. F. Davies, F. H. Marshall, and J. P. Reid (2013), Measurements of the sensitivity of aerosol hygroscopicity and the kappa parameter to the O/C ratio, *J. Phys. Chem. A*, *117*(51), 14,120–14,131, doi:10.1021/jp407991n.
Sachse, G. W., G. F. Hill, L. O. Wade, and M. G. Perry (1987), Fast-response, high-precision carbon-monoxide sensor using a tunable diode laser absorption technique, *J. Geophys. Res.*, *92*(D2), 2071–2081, doi:10.1029/JD092iD02p02071.
Sachse, G. W., J. E. Collins, G. F. Hill, L. O. Wade, L. G. Burney, and J. A. Ritter (1991), Airborne tunable diode-laser sensor for high-precision concentration and flux measurements of carbon dioxide and methane, *Meas. Atmos. Gases*, *1433*, 157–166, doi:10.1117/12.46162.
Saide, P. E., et al. (2015), Revealing important nocturnal and day-to-day variations in fire smoke emissions through a multiplatform inversion, *Geophys. Res. Lett.*, *42*, 3609–3618, doi:10.1002/2015GL063737.
Samset, B. H., et al. (2014), Modelled black carbon radiative forcing and atmospheric lifetime in AeroCom Phase II constrained by aircraft observations, *Atmos. Chem. Phys.*, *14*(22), 12,465–12,477, doi:10.5194/acp-14-12465-2014.
Schwarz, J. P., et al. (2008), Measurement of the mixing state, mass, and optical size of individual black carbon particles in urban and biomass burning emissions, *Geophys. Res. Lett.*, *35*, L13810, doi:10.1029/2008GL033968.
Schwarz, J. P., J. R. Spackman, R. S. Gao, L. A. Watts, P. Stier, M. Schulz, S. M. Davis, S. C. Wofsy, and D. W. Fahey (2010), Global-scale black carbon profiles observed in the remote atmosphere and compared to models, *Geophys. Res. Lett.*, *37*, L18812, doi:10.1029/2010GL046007.
Schwarz, J. P., B. H. Samset, A. E. Perring, J. R. Spackman, R. S. Gao, P. Stier, M. Schulz, F. L. Moore, E. A. Ray, and D. W. Fahey (2013), Global-scale seasonally resolved black carbon vertical profiles over the Pacific, *Geophys. Res. Lett.*, *40*, 5542–5547, doi:10.1002/2013GL057775.
Schwarz, J. P., A. E. Perring, M. Z. Markovic, R. S. Gao, S. Ohata, J. Langridge, D. Law, R. McLaughlin, and D. W. Fahey (2015), Technique and theoretical approach for quantifying the hygroscopicity of black-carbon-containing aerosol using a single particle soot photometer, *J. Aerosol Sci.*, *81*, 110–126, doi:10.1016/j.jaerosci.2014.11.009.
Shen, Z., J. Liu, L. W. Horowitz, D. K. Henze, S. Fan, H. Levy II, D. L. Mauzerall, J. T. Lin, and S. Tao (2014), Analysis of transpacific transport of black carbon during HIPPO-3: Implications for black carbon aging, *Atmos. Chem. Phys.*, *14*(12), 6315–6327, doi:10.5194/acp-14-6315-2014.
Shingler, T., et al. (2016a), Airborne characterization of subsaturated aerosol hygroscopicity and refractive index from the surface to 6.5 km during the SEAC^{4}RS campaign, *J. Geophys. Res. Atmos.*, *121*, 4188–4210, doi:10.1002/2015JD024498.
Shingler, T., et al. (2016b), Ambient observations of hygroscopic growth factor and f(RH) below 1: Case studies from surface and airborne measurements, *J. Geophys. Res. Atmos.*, *121*, 13,661–13,677, doi:10.1002/2016JD025471.
Sorooshian, A., S. Hersey, F. J. Brechtel, A. Corless, R. C. Flagan, and J. H. Seinfeld (2008), Rapid, size-resolved aerosol hygroscopic growth measurements: Differential aerosol sizing and hygroscopicity spectrometer probe (DASH-SP), *Aerosol Sci. Technol.*, *42*(6), 445–464, doi:10.1080/02786820802178506.
Stein, A. F., R. R. Draxler, G. D. Rolph, B. J. B. Stunder, M. D. Cohen, and F. Ngan (2015), NOAA'S HYSPLIT atmospheric transport and dispersion modeling system, *Bull. Am. Meteorol. Soc.*, *96*(12), 2059–2077, doi:10.1175/bams-d-14-00110.1.
Suda, S. R., et al. (2014), Influence of functional groups on organic aerosol cloud condensation nucleus activity, *Environ. Sci. Technol.*, *48*(17), 10,182–10,190, doi:10.1021/es502147y.
Taylor, J. W., et al. (2014), Size-dependent wet removal of black carbon in Canadian biomass burning plumes, *Atmos. Chem. Phys.*, *14*(24), 13,755–13,771, doi:10.5194/acp-14-13755-2014.
Toon, O., et al. (2016), Planning, implementation and scientific goals of the Studies of Emissions and Atmospheric Composition, Clouds, Climate Coupling by Regional Surveys (SEAC4RS) field mission, *J. Geophys. Res. Atmos.*, *121*, 4967–5009, doi:10.1002/2015JD024297.
Wang, Q., D. J. Jacob, J. R. Spackman, A. E. Perring, J. P. Schwarz, N. Moteki, E. A. Marais, C. Ge, J. Wang, and S. R. H. Barrett (2014), Global budget and radiative forcing of black carbon aerosol: Constraints from pole-to-pole (HIPPO) observations across the Pacific, *J. Geophys. Res. Atmos.*, *119*, 195–206, doi:10.1002/2013JD020824.
Wisthaler, A., A. Hansel, R. R. Dickerson, and P. J. Crutzen (2002), Organic trace gas measurements by PTR-MS during INDOEX 1999, *J. Geophys. Res.*, *107*(D19), doi:10.1029/2001JD000576.
Wonaschuetz, A., et al. (2013), Hygroscopic properties of smoke-generated organic aerosol particles emitted in the marine atmosphere, *Atmos. Chem. Phys.*, *13*(19), 9819–9835, doi:10.5194/acp-13-9819-2013.
Zhang, J., J. Liu, S. Tao, and G. A. Ban-Weiss (2015), Long-range transport of black carbon to the Pacific Ocean and its dependence on aging timescale, *Atmos. Chem. Phys.*, *15*(20), 11,521–11,535, doi:10.5194/acp-15-11521-2015.
Zhang, R., A. F. Khalizov, J. Pagels, D. Zhang, H. Xue, and P. H. McMurry (2008), Variability in morphology, hygroscopicity, and optical properties of soot aerosols during atmospheric processing, *Proc. Natl. Acad. Sci. U.S.A.*, *105*(30), 10,291–10,296, doi:10.1073/pnas.0804860105.